

Spin-glass transition in single-crystal BiFeO₃Manoj K. Singh,¹ W. Prellier,² M. P. Singh,² Ram S. Katiyar,^{1,*}† and J. F. Scott^{3,*}‡¹*Department of Physics and Institute of Functional Nano materials, University of Puerto Rico, Puerto Rico 00931-3343, USA*²*Laboratoire CRISMAT, CNRS UMR 6508, ENSICAEN, 6 Boulevard du Maréchal Juin, F-14050 Caen Cedex, France*³*Department of Earth Science, University of Cambridge, Cambridge CB2 3EQ, United Kingdom*

(Received 17 September 2007; revised manuscript received 7 January 2008; published 2 April 2008)

Magnetic properties of BiFeO₃ (BFO) single crystals with rhombohedral symmetry (*R3c*) were measured in the temperature range of 4.2–350 K. Zero field cooled (ZFC) and field cooled magnetization curves split below 250 K with a sharp cusp around 50 K in the ZFC curves revealing spin-glass behavior in BFO single crystals. The observed coercive field increases with decreasing temperature, suggesting weak ferromagnetism below ~ 10 K and spin glass behavior below ~ 120 K. The cusps around the freezing temperature [$T_f(\omega)$] which are frequency dependent confirm the spin-glass behavior in BFO single crystals with spin freezing temperature ($T_{SG}=29.4 \pm 0.2$ K). The critical exponent $z\nu=1.38$ agrees rather well with experimental values in LaMn_{0.5}Fe_{0.5}O₃ ($z\nu=1.0$) [K. De *et al.*, J. Appl. Phys. **99**, 13908 (2006)] and the mean field theory ($z\nu=2.0$) of Kirkpatrick and Sherrington [Phys. Rev. B **17**, 4384 (1970)].

DOI: 10.1103/PhysRevB.77.144403

PACS number(s): 75.50.Lk, 75.40.Gb

I. INTRODUCTION

Magnetoelectric materials that are multiferroic exhibit ferroelectric (or antiferroelectric) properties in combination with the ferromagnetic (or antiferromagnetic) properties.^{1–3} However, the ground states are not necessarily coupled, but they might exhibit various novel properties, such as a variation in the remanent electrical polarization under applied magnetic fields or magnetization change under applied electric fields. BiFeO₃ (BFO) is known to be one of very few materials that exhibit multiferroism at room temperature.

Bulk BiFeO₃ is a rhombohedrally distorted ferroelectric perovskite ($T_c \approx 1100$ K) with the space group *R3c* (Ref. 4). The rhombohedral unit cell parameters are $a=5.63$ Å and $\alpha=89.35^\circ$. BiFeO₃ shows *G*-type antiferromagnetism up to 643 K (T_N),⁵ where all the neighboring magnetic moments are oriented antiparallel to each other. In addition, the axis along which the spin are aligned rotates throughout the crystal, resulting in a spiral spin structure with a large period of ~ 620 Å, which is incommensurate with the lattice parameter.^{4,5} The existence of modulated magnetic structure in BFO has been experimentally confirmed by neutron diffraction, Mössbauer spectroscopy, NMR, and EPR studies but with some controversies.^{4–8}

The magnetic structure of BiFeO₃ is different from other antiferromagnets in that the inversion symmetry is absent in this crystal and magnetic structure. This circumstance produces unusual properties, such as modulated magnetic structure and a linear magnetoelectric effect with weak ferromagnetism.⁹ The linear magnetoelectric effect in BFO is also an important physical property, and according to Refs. 10–12, it disappears in the presence of modulated magnetic ordering with *R3c* structure. However, the spiral component and modulated structure are absent in thin films, resulting in weak ferromagnetism¹³ and an antisymmetric magnetoelectric tensor $\alpha_{21}=-\alpha_{12}$. Wang *et al.*¹⁴ fabricated BFO films that exhibited enhanced thickness-dependent magnetism compared to the bulk. A more recent study, however, argues¹⁵ that this compressive epitaxial strain does not enhance the

magnetization in BFO. The weak ferromagnetism in BFO was originally inferred by Smolenskii and Yudin¹⁶ but it also remains controversial. In order to study the magnetic properties of BFO at low temperature, Nakamura *et al.*¹⁷ predicted a spin-glass freezing behavior in BFO at low temperatures. In recent years, several authors report the magnetic behavior of BFO at low temperature and observe a dramatic change below 200 K.^{18–20} As an example, Park *et al.*²⁰ inferred that the anomalous magnetization behavior in BFO nanoparticles arises from a complex interplay between the finite size effects, interparticle interaction, and a random distribution of anisotropy axis in nanoparticle assemblies.

In this paper, we investigate the magnetic properties of BFO single crystal grown by flux method. The observed zero field cooled (ZFC) and field cooled (FC) magnetization curves reveal a spin-glass behavior at low temperatures. The spin-glass behavior in BFO is also supported by the observation of a cusp at the freezing temperature, which decreases with increasing frequencies in the ac susceptibility data. The magnetization in BFO was measured with an applied magnetic field, and the results indicate weak ferromagnetism in BFO at 5 K.

II. EXPERIMENTAL DETAILS

A single crystal of BiFeO₃ was prepared by employing a flux method. The flux materials Bi₂O₃ and Fe₂O₃ were mixed and annealed in a platinum crucible at 820 °C for 12 h in air. After annealing, the melt was cooled to 720 °C at a rate of 1 °C/h with continuous rotation of crucible with 30 rpm. Many pieces of the single crystal with a pseudocubic dimension of $1.0 \times 1.0 \times 0.5$ mm³ were obtained. To examine the structure and orientation of the BFO single crystal, x-ray diffraction (XRD) experiments of polycrystalline powder (obtained by crushing the single crystal) and BFO single crystal were carried out, and their results are shown in Figs. 1(a) and 1(b), respectively. As presented in Fig. 1(a), the crystals display a rhombohedral (hexagonal) structure without any impurity phase. The XRD pattern of the major phase

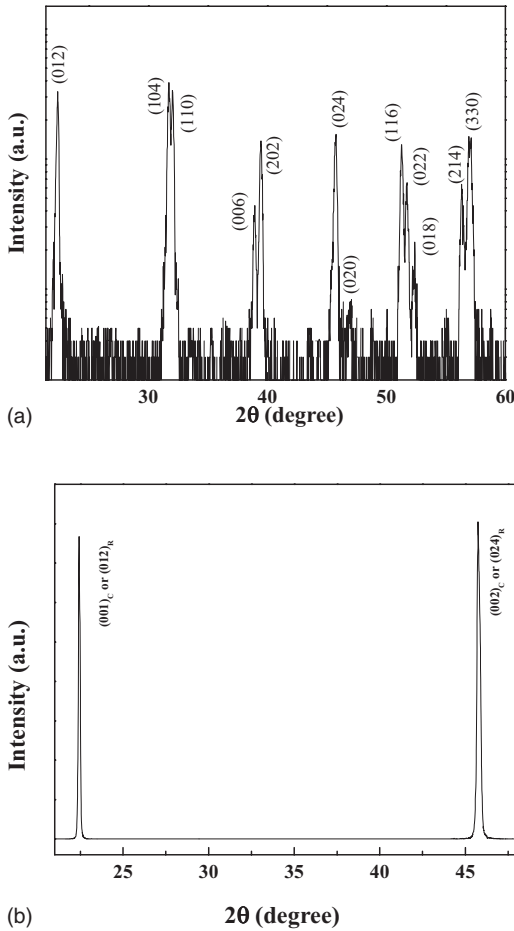


FIG. 1. (a) θ - 2θ XRD pattern of a polycrystalline BiFeO_3 (obtained by crushing the single crystal). (b) $(\theta$ - 2θ) XRD pattern of major phase of BiFeO_3 single crystal.

of single crystal is exclusively characterized by the $[001]_{\text{cubic}}$ or $[012]_{\text{rhombohedral}}$ reflections, as presented in Fig. 1(b). For the magnetization measurements, we have used a superconducting quantum interface device based magnetometer (Quantum Design MPMS-5). These measurements were carried out by cooling the sample to the desired temperature in the presence or absence of applied magnetic field. The orientations of magnetic field during the field cooled measurement remain the same.

III. EXPERIMENTAL RESULTS AND ANALYSIS

A. dc susceptibility

Figure 2 displays the ZFC and FC magnetizations of the BFO single crystal. These measurements were performed utilizing 10 000 Oe magnetic field. During the measurements, an external magnetic field of 10 kOe (1 T) was applied parallel to the $[111]_c$ direction. The magnetization induced along the in-plane direction which is perpendicular to $[111]_c$ (i.e., $[001]_h$) was measured because the magnetization easy axis of $R3c$ BFO is parallel to $[110]_h$ which is vertical to $[001]_h$.¹² As seen in Fig. 2 recorded in the temperature range of 350–150 K, the ZFC and FC magnetization values de-

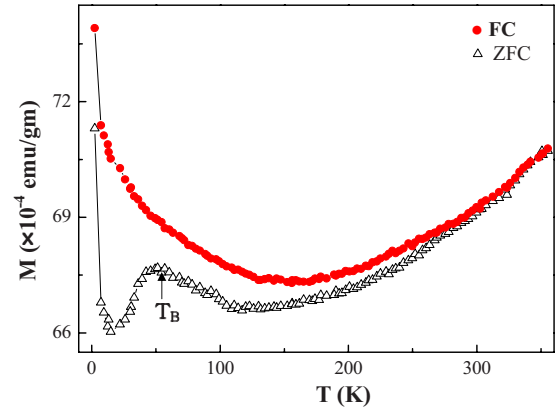


FIG. 2. (Color online) Temperature dependence of the dc magnetization (ZFC and FC) of BiFeO_3 single crystal.

crease with decreasing the temperature, which is consistent with conventional antiferromagnetic material. The ZFC and FC curves start to split below 250 K and a divergence between the ZFC and FC magnetization curves increases with decreasing the temperature. The splitting of ZFC and FC magnetizations at low temperature reveals spin-glass transition in BFO single crystal. As the temperature decreases below ~ 150 K, ZFC and FC magnetizations increase gradually with decreasing temperature, and ZFC shows an anomalous behavior below 100 K. These experimental results indicate that a change in spin ordering at low temperature may be due to spin reorientation in BiFeO_3 single crystal like other orthoferrites.^{21,22}

The behaviors of magnetization with temperature are good agreement with electromagnon in study in BFO single crystal.^{23,24} In Ref. 23, we find that in the monoclinic magnetic phase (rhombohedral crystallographic phase), we see both sigma (ferromagnetic magnon) and gamma (antiferromagnetic magnon) modes at 18.3 and 26.4 cm^{-1} (80 K), and that they are very similar to those two branches in orthoferrites such as ErFeO_3 .²¹ However, at exactly 200 K, there is an abrupt change in the frequency and intensity of the sigma mode, and the gamma mode disappears. This suggests a spin reorientation, as is common in orthoferrites. Therefore, there appear to be subtle and unpredicted magnetic changes going on in the region of 200 K, far below $T_N=640$ K and these may influence the spin-glass behavior we see initially on cooling at 120 K.

In the ZFC curve, we also observed a sharp cusp around 50 K, which is similar to the observed blocking temperature T_B in antiferromagnetic material $\gamma\text{-Fe}_2\text{O}_3$ at 72 K.²⁵ This temperature is defined as a typical blocking process of an assembly of superparamagnetic spins and is qualitatively related to the presence of small particles, domains or domain walls in the system.²⁵ Similar features in the ZFC and FC magnetization curves at low temperature were reported recently in bulk and in 245 nm particle size of BFO.²⁰ Both curves (FC and ZFC) show sudden jumps in magnetization at 5 K, indicating a weak ferromagnetic behavior in BFO single crystal.

B. ac susceptibility

In order to understand the origin of the spin-glass behavior and the freezing temperature as observed in dc magneti-

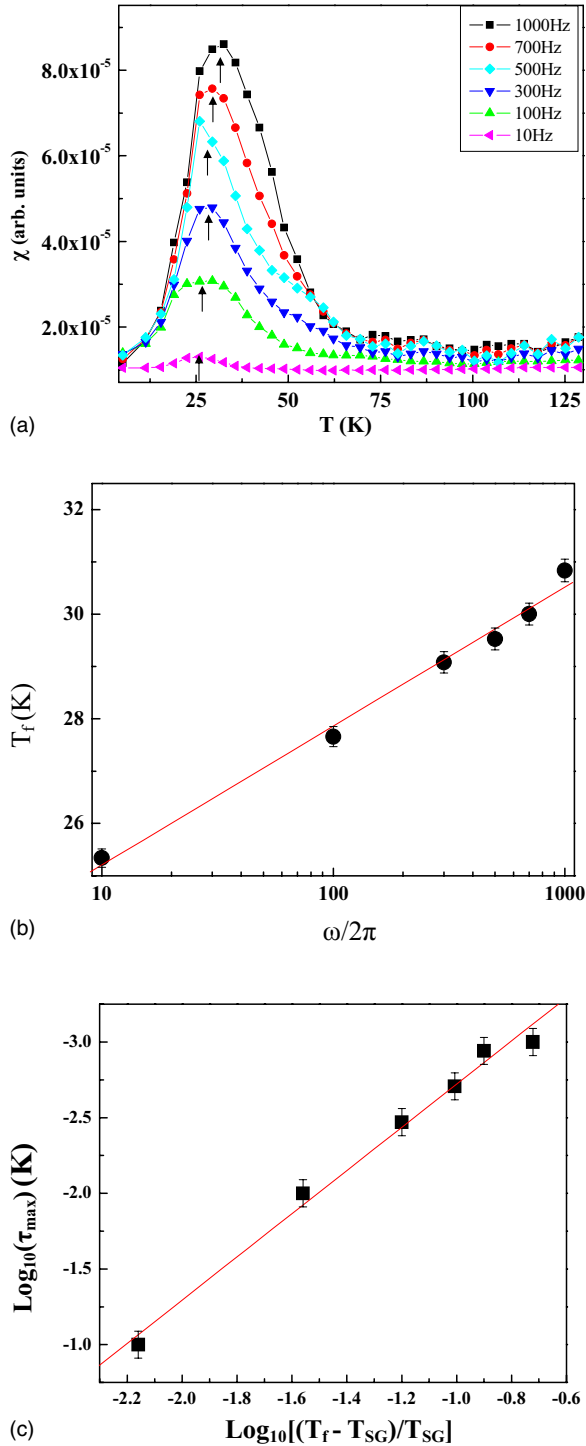


FIG. 3. (Color online) (a) Temperature dependent ac susceptibility (magnitude) $\chi(T) = \sqrt{(\chi')^2 + (\chi'')^2}$ of BiFeO₃ single crystal under different frequencies from 10 to 1000 Hz. (b) $T_f(\omega)$ is plotted as a function of $\log \omega$. (c) $\log_{10} f$ is plotted as a function of $\log_{10}[(T_f - T_{SG})/T_{SG}]$.

zation data (also predicted in Refs. 17–20), we measured the ac susceptibility of BiFeO₃ single crystal with varying the frequencies (f) from 10 to 100, 300, 500, 700, and 1000 Hz. In a spin glass system, a magnetic spin experiences random interaction with other magnetic spins, resulting in a state that

is highly irreversible and metastable. The ac susceptibility measurement is particularly important for spin glasses because it determines the freezing temperature accurately.^{26,27} The magnitude $\chi(T)$, real component $\chi'(T)$ (in phase), the imaginary component $\chi''(T)$ (out of phase), and ac susceptibility were measured as a function of frequency (Figs. 3 and 4). From ac susceptibility measurements, we observed that at low temperature $\chi(T)$, $\chi'(T)$, and $\chi''(T)$ curves exhibited a sharp peak at spin glass transition temperature $T_f(\omega)$, which is frequency dependent. The observed nonzero out-of-phase component in $\chi(T)$ below the spin glass freezing temperature is due to the irreversibility in the spin glass. The peak temperature $T_f(\omega)$ shifts toward higher temperatures, and the height of frequency cusps increases with increasing frequency. The location of the peaks is dependent on the frequency of the ac susceptibility measurement, a feature that is not present in any other antiferromagnetic or ferromagnetic long-range order system; thus, it confirms the spin glass behavior of BFO single crystal. From Figs. 4(a) and 4(b), the $T_f(\omega)$ values for observed cusps in $\chi'(T)$ are found to be slightly higher than $\chi''(T)$, which is very common in conventional spin-glass systems. The most important result of the ac susceptibility measurement is the negative cusps at T_f in the imaginary of ac susceptibility $\chi''(T)$ [Fig. 4(b)], which may arise from the modulated magnetic structure. Such behavior was also reported for in the superconductor materials but was not observed in conventional spin glass materials. In addition, we also observed small cusps in susceptibility measurement between temperature range of 50–80 K for higher applied frequencies (>500 Hz). These cusps are may be originate from the superparamagnetic spins in the system, as we observed in ZFC measurement in Fig. 2. The low-temperature resistivity of BiFeO₃ is about $10^9 \Omega \text{ cm}$, and the dielectric constant is about 50. Therefore, including the permittivity of free space, the RC-time constant for BiFeO₃ specimens is close to 0.03 s, independent of geometry. Hence, a mechanical resonance is expected near $f=30$ Hz, exactly in the middle of our measurement range. This could be responsible for the increase in ac susceptibility with increasing frequency.

The value of the frequency sensitivity K of $T_f(\omega)$ has been used as a possible distinguishing factor for the presence of spin-glass phase and is defined as in Refs. 26 and 27. $K = \Delta T_f / T_f \Delta \log \omega$ and $T_f(\omega)$ vs $\log \omega$ are shown in Fig. 3(b). The calculated K value for BFO single crystal is 0.0144, which is higher than the conventional spin-glass system ($\sim 10^{-2} - 10^{-3}$) but slightly smaller than the superparamagnetic state ($10^{-1} - 10^{-2}$).²⁷ Using these criteria, we conclude that the BFO single crystal belongs to a different class of spin glass material. In order to study the critical temperature for spin glass nature in this system, we utilized the conventional critical spin dynamics.^{28,29} This dependence of $T_f(\omega)$ on frequency (f) is well described by the conventional critical “slowing down” of the spin dynamics²⁹ as described by

$$\frac{\tau}{\tau_0} \propto \left(\frac{T_f - T_{SG}}{T_{SG}} \right)^{-z\nu}, \quad (1)$$

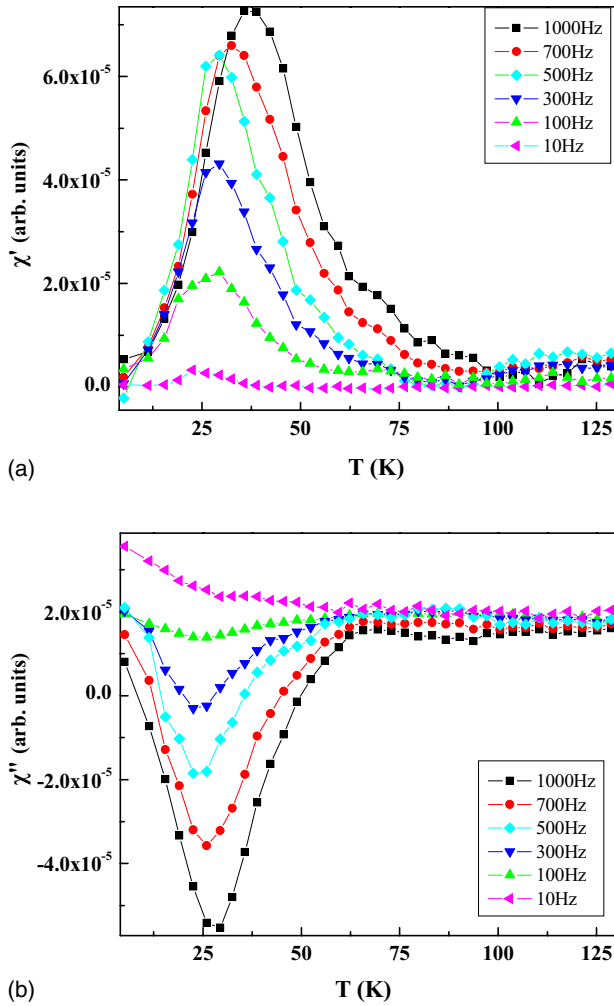


FIG. 4. (Color online) (a) Temperature dependence of in phase ac susceptibility $\chi'(T)$ of BiFeO₃ single crystal under different frequencies from 10 to 1000 Hz. (b) Temperature dependence out of phase ac susceptibility $\chi''(T)$ of BiFeO₃ single crystal under different frequencies from 10 to 1000 Hz.

where $\tau \propto f^{-1}$, T_{SG} is the critical temperature for spin glass ordering which is equivalent to the $T_f(\omega)$ at $f \rightarrow 0$, $z\nu$ is a constant component, and τ_0 is the characteristic time scale for the spin dynamics. The agreement with Eq. (1) is shown in Fig. 2(c), where $\log_{10} f$ is plotted as a function of $\log_{10}[(T_f - T_{SG})/T_{SG}]$. The best fit to the form shown in Eq. (1) is obtained by choosing the value of critical temperature for spin glass ordering $T_{SG} = 29.4 \pm 0.2$ K, which minimized the least square deviation from a straight line fit. The value of $\log_{10} \tau_0 = 4.1 \pm 0.1$ and $z\nu = 1.4 \pm 0.2$ are then extracted from the intercept and the slope, respectively. The observed $z\nu$ for BiFeO₃ single crystal is very similar to those in La_{0.5}Mn_{0.5}FeO₃, which is characterized as a non classical spin glass compounds.³⁰

BiFeO₃ is not a conventional ferromagnet or antiferromagnet, but rather a G -type long-range wavelength spiral; therefore, the dynamic exponent $z\nu$ describing its spin glass behavior might be expected to differ from that of 9.0–10.0 found experimentally³¹ or 7.0–8.0 found theoretically³² for Ising systems. Our value of 1.38 is much closer to that of 2.0

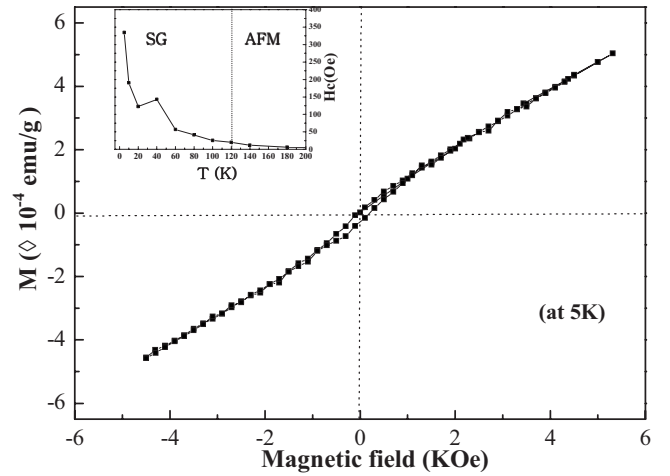


FIG. 5. Magnetization as a function of external magnetic field at $T = 5$ K. The inset shows the temperature dependence of the coercive field.

known for mean field or hydrodynamic models,³³ which may be due to the long-range Coulombic contributions to the electromagnons, which are not pure spin waves.^{22,23} Exponents due to diffusion are also not unreasonable since both Ogielski³¹ and S. Kirkpatrick and co-workers³² argued that the physical mechanism responsible for Eq. (1) is diffusion. In this respect, we note that the negative cusp in susceptibility is also highly unusual among magnetic spin glasses and is more reminiscent of phenomena in superconductors. This might also arise from spin diffusion. We note parenthetically that creep in other ferroelectrics has been described in terms of critical exponents varying from ($\mu = 0.5 - 1.0$)³³ and that a diffusion model was shown to be applicable in such cases. Hence, a possible interpretation of our exponent $z\nu$ is that it arises from the diffusion of domain walls. The domain walls in BiFeO₃ are known to involve both ferroelectric and ferromagnetic properties.³⁴ The magnetic domain walls in magnetoelectric, multiferroic materials, such as BiFeO₃, are complicated and can in general be electrically charged, as shown by Mostovoy.³⁵

C. Magnetic hysteresis curve

The magnetization of BFO single crystal as a function of magnetic field $M(H)$ under the ZFC at various temperatures have also been measured. At higher temperatures, the magnetization curves show the antiferromagnetic feature, as expected. The $M-H$ curve deviates from a linear relation and bends more as temperature decreases below the freezing temperature. The experimentally observed $M-H$ curve at 5 K and the coercive field at different temperatures are shown, respectively, in Fig. 5 and its inset. The observed $M-H$ curve at 5 K reveals weak ferromagnetism in BFO single crystals due to spin freezing. It is also observed in the hysteresis curve at 5 K, which did not show the saturation in fields up to 6000 Oe like other conventional spin glass systems. We also observed that the coercive field increases gradually below ~ 120 K and abruptly below spin freezing temperature ($\sim T_{SG}$) with decreasing the temperature. This indicates an

intrinsic magnetic transition in this system at low temperatures because in conventional antiferromagnets or ferromagnets, the coercive field is attributed to the blocking of the domain wall motion.

IV. CONCLUSION

We measured the ZFC and FC magnetizations, and magnetizations, and magnetization (M - H) in BFO single crystal with rhombohedral symmetry $R3c$ and inferred spin-glass behavior below 120 K. The spin-glass ordering in BFO single crystal was also confirmed by the ac susceptibility measurements, in which the observed peak temperature $T_f(\omega)$ shifted toward higher temperature with increasing frequency. The observed ac susceptibility data suggested that a mean-field hydrodynamics diffusion model may be applicable to explain the spin glass transition in BFO single crys-

tal. The magnetization and coercive measurements also revealed spin-glass nature and weak ferromagnetism in BFO below $T_{SG}=29.4 \pm 0.2$ K.

A final question concerns the ratio of Néel temperature to spin-glass temperature. Campbell and co-workers showed that this should be 1.5:1 for Ising models. However, in bismuth ferrite, we suggest that the system is not Ising-like and note that our values of $T(\text{Néel})$ and $T(\text{spin glass})$ are very similar to those in YFeO₃.²²

ACKNOWLEDGMENTS

We gratefully acknowledge the financial support from the DOD Grant Nos. W911NF-06-1-0030 and W911NF-06-1-0183. Experimental measurement of this work is carried out in the frame of the NoE FAME (FP6-500159-1) and the STREP MaCoMuFi (NMP3-CT-2006-033221) supported by the European Community and by the CNRS, France.

*Corresponding authors.

†rkatiyar@speclab.upr.edu

‡jsco99@esc.cam.ac.uk

¹N. A. Hill, *J. Phys. Chem. B* **104**, 6694 (2000).

²W. Eerenstein, N. D. Mathur, and J. F. Scott, *Nature (London)* **442**, 759 (2006).

³M. Fiebig, Th. Lottermoser, D. Fröhlich, A. V. Goltsev, and R. V. Pisarev, *Nature (London)* **419**, 818 (2002).

⁴P. Fischer, M. Połomska, I. Sosnowska, and M. Szymański, *J. Phys. C* **13**, 1931 (1980).

⁵C. Michel, J.-M. Moreau, G. D. Achenbach, R. Gerson, and W. J. James, *Solid State Commun.* **7**, 701 (1969).

⁶J. R. Teague, R. Gerson, and W. J. James, *Solid State Commun.* **8**, 1073 (1970).

⁷A. J. Jacobson and B. E. F. Fender, *J. Phys. C* **8**, 844 (1975).

⁸R. Przeniosło, A. Palewicz, M. Reguński, I. Sosnowska, R. M. Ibberson, and K. S. Knight, *J. Phys.: Condens. Matter* **18**, 2069 (2006).

⁹A. M. Kadomtseva, A. K. Zvezdin, Y. F. Popov, A. P. Pyatakov, and G. P. Vorob'ev, *JETP Lett.* **79**, 11 (2004).

¹⁰I. Sosnowska, T. Peterlin-Neumaier, and E. Steichele, *J. Phys. C* **15**, 4815 (1982).

¹¹C. Tabares-Munoz *et al.*, *Jpn. J. Appl. Phys., Part 1* **24**, 1051 (1985).

¹²B. Ruetter, S. Zvyagin, A. P. Pyatakov, A. Bush, J. F. Li, V. I. Belotelov, A. K. Zvezdin, and D. Viehland, *Phys. Rev. B* **69**, 064114 (2004).

¹³H. Bea, M. Bibes, S. Petit, J. Kreisel, and A. Barthelemy, *Philos. Mag. Lett.* **87**, 165 (2007).

¹⁴J. Wang *et al.*, *Science* **299**, 1719 (2003).

¹⁵W. Eerenstein, F. D. Morrison, J. Dho, M. G. Blamire, J. F. Scott, and N. D. Mathur, *Science* **307**, 1203a (2005).

¹⁶G. A. Smolenskii and V. M. Yudin, *Sov. Phys. Solid State* **5**, 2525 (1965).

¹⁷S. Nakamura, S. Soeya, N. Ikeda, and M. Tanaka, *J. Appl. Phys.*

74, 5652 (1993).

¹⁸R. Mazumdar, S. Ghosh, P. Mondal, D. Bhattacharya, S. Dasgupta, N. Das, A. Sen, A. K. Tyagi, M. Sivakumar, T. Takami, and H. Ikuta, *J. Appl. Phys.* **100**, 033908 (2006).

¹⁹H. Naganuma, and S. Okamura, *J. Appl. Phys.* **101**, 09M103 (2007).

²⁰T. J. Park, G. C. Papaefthymiou, A. J. Viescas, A. R. Moodenbaugh, and S. S. Wong, *Nano Lett.* **7**, 766 (2007).

²¹N. Koshizuka and S. Ushioda, *Phys. Rev. B* **22**, 5394 (1980).

²²Yu. G. Chukalkin and B. N. Goshchitskii, *Phys. Status Solidi A* **200**, R9 (2003).

²³M. K. Singh, R. S. Katiyar, and J. F. Scott, arXiv:0712.4040 (unpublished).

²⁴M. Cazayous, Y. Gallais, A. Sacuto, R. De Sousa, D. Lebeugle, and D. Colson, arXiv:0712.3044 (unpublished).

²⁵B. Martinez, X. Obradors, L. Balcells, A. Rouanet, and C. Monty, *Phys. Rev. Lett.* **80**, 181 (1998).

²⁶J. A. Mydosh, *J. Magn. Magn. Mater.* **158**, 606 (1996).

²⁷J. A. Mydosh, *Spin Glass: An Experimental Introduction* (Taylor & Francis, London, 1993).

²⁸P. C. Hohenberg and B. I. Halperin, *Rev. Mod. Phys.* **49**, 435 (1977).

²⁹K. Gunnarsson, P. Svedlindh, P. Nordblad, and L. Lundgren, *Phys. Rev. Lett.* **61**, 754 (1988).

³⁰K. De, M. Thakur, A. Manna, and S. Giri, *J. Appl. Phys.* **99**, 013908 (2006).

³¹A. T. Ogielski, *Phys. Rev. B* **32**, 7384 (1985).

³²S. Kirkpatrick and D. Sherrington, *Phys. Rev. B* **17**, 4384 (1970); I. A. Campbell, *ibid.* **33**, 3587 (1986).

³³P. Berge, P. Calmetter, C. Laj, M. Tournarie, and B. Volochine, *Phys. Rev. Lett.* **24**, 1223 (1970).

³⁴G. Catalan, H. Bea, S. Fusil, M. Bibes, P. Paruch, A. Barthelemy, and J. F. Scott, *Phys. Rev. Lett.* **100**, 027602 (2008).

³⁵M. Mostovoy, *Phys. Rev. Lett.* **96**, 067601 (2006).